Arabidopsis sculpt distinct root-associated microbiomes through the synthesis of secondary metabolites and defense signaling molecules

Enoch Narh Kudjordjie
Aarhus Universitet
Rumakanta Sapkota
Aarhus Universitet
Mogens Nicolaisen (mn@agro.au.dk)
Aarhus Universitet https://orcid.org/0000-0002-0407-2488

Research

Keywords: Plant microbiomes, defense signaling pathways, plant metabolites, glucosinolates, flavonoids, phytohormones

Posted Date: May 14th, 2020

DOI: https://doi.org/10.21203/rs.3.rs-27655/v1

Arabidopsis sculpt distinct root-associated microbiomes through the synthesis of secondary metabolites and defense signaling molecules

Enoch Narh Kudjordjie[1], Rumakanta Sapkota[1, 2], Mogens Nicolaisen[1]

[1]Aarhus University, Faculty of Technical Sciences, Department of Agroecology, Forsøgsvej 1, DK4200, Slagelse Denmark.

[2]Current address: Aarhus University, Faculty of Technical Sciences, Department of Environmental Science, Frederiksborgvej 399, 4000 Roskilde.

Corresponding author: mn@agro.au.dk

Abstract

Background

Plant mutants with alterations in specific biosynthetic or signaling pathways exhibit distinct biochemical or physiological traits and are, thus, suitable models for studying links between the plant and its associated microbiota. Here, we examined microbial community structures of a range of *Arabidopsis thaliana* mutants disrupted in metabolic pathways for the production of glucosinolates, flavonoids, or a number of defense signaling molecules. Arabidopsis mutants and their background wild types (controls) were grown in natural soil and maintained in a greenhouse for 4 weeks before collection of roots for microbiome analysis. We characterized bacterial and fungal communities using 16S rRNA and fungal ITS amplicon sequencing, respectively.

Results

Our results showed that the Arabidopsis mutants had distinct microbial profiles compared to control plants. The relative abundances of the bacterial classes Actinobacteria, Thermoleophilia and Verrucomicrobiae, and the fungal classes Eurotiomycetes and Sordariomycetes were the most affected when comparing mutants and their wild types. At the genus level, the bacterial taxa *Azospirillum*, *Fluviicola*, and *Flavobacterium* were significantly enriched in most glucosinolate, flavonoid and signaling mutants while the fungal taxa *Sporobolomyces* and *Emericellopsis* were enriched in several glucosinolate and defense signaling mutants.

Conclusion

By using different Arabidopsis mutants and their background controls, we showed that plant secondary metabolism and defense signaling molecules affect bacterial and fungal community structures. We conclude that disruption of pathways for secondary metabolite production or disruption of defense signaling pathways affected the innate mechanisms that modulate plant root-associated microbiome assembly.

Keywords: Plant microbiomes, defense signaling pathways, plant metabolites, glucosinolates, flavonoids, phytohormones

Introduction

Plants interact with a vast diversity of microorganisms both above and belowground, and the outcomes of these interactions may be commensal, beneficial or detrimental to the plant. Essentially, the plant employs a range of strategies such as the action of preformed and/or induced chemical compounds in combination with the plant innate immune systems to sculpt the microbiota (1, 2).

Plant secondary metabolites such as glucosinolates (GLS) and flavonoids (FLVs) have been widely studied for several microbiota-mediating and plant protective functions (3**,** 4). For instance, GLS from the roots of Brassica species were found to inhibit microbial pathogens including *Pseudomonas syringae, Alternaria brassicicola, Gaeumannomyces graminis, Botrytis cinerea, Fusarium oxysporium* and *Peronospora parasitica* (5, 6). The FLVs are well known for their chemoattractant and signaling function in legume-rhizobia interactions resulting in N-fixation (7,8). FLVs also possess antimicrobial activity used in defense against pathogens. They are involved in plant-mycorrhizal associations, and act as enhancers of bacterial growth rates (7, 8). The activation of the innate plant immune system is inevitable due to the constant interaction between plants and microbes (1). The plant immune system, which is highly networked with other defense repertoires, is under constant activation by perception of microbial associated molecular patterns resulting in a broad spectrum of inducible defense responses (9). Plant hormones serve as signaling molecules in regulating the innate immune network. Phytohormones including salicylic acid (SA), jasmonic acid (JA), ethylene (ET) and abscisic acid (ABA) act as molecular switches in stimulating inducible defense against biotic and abiotic stresses (9). Owing to its robust and overarching activation of defense repertoires, the immune system is perceived to affect microbial community structures (10).

The biosynthetic pathways and genes involved in GLS (11,12,13), FLV (14,15,16) and defense signaling (17,18,19) are well described, and research is directed towards exploiting these pathways to study the links between plant gene functions and microbiome assemblage. Several well-characterized mutants of the model plant, *Arabidopsis thaliana* (hereafter Arabidopsis) have become quintessential for studying this relationship. For example, Badri *et al.* (20) reported effects on microbial communities of a mutation in a plant ATP transporter involved in exudation of plant secondary metabolites, and further concluded that individual plant genes are actively involved in the interaction with microbial communities. By using GLS (21), FLV (20) and benzoxazinoid (BX)

mutants (22,23), the influence of plant defensive secondary metabolites on the plant-associated microbiota has been demonstrated. For example, distinct microbiomes were observed in maize parental lines and their isogenic mutants (bx1, bx2 and bx6) carrying disruptions in genes encoding enzymes in different steps of the BX pathway (23). This study further demonstrated a gatekeeper role of BXs in modulating plant-associated microbiomes associated with plant roots. In other studies, the coumarin-impaired mutants, myb72-2, bglu42 and f6'h1 were used to demonstrate the impact of coumarin on microbial community assembly (24–26). In addition, studies have used Arabidopsis mutants to examine the influence of phytohormones on microbial community structures (27,28).

Mechanistic processes at the rhizoplane, including the gating role of plant secondary metabolites (23) and defense signaling molecules (DSMs) (27,28), are controlling the assembly of host specific-microbiomes. We hypothesized that mutations in pathways for the synthesis of certain secondary metabolites and DSMs disrupt the ability of the plant to sculpt its associated microbiome. While it is evident that single plant metabolites or DSMs affect host-associated microbiomes, studies that characterize the effect of a range of these chemical compounds on both bacterial and fungal microbiomes under similar and natural conditions are scarce. Such a comprehensive analysis using plant mutants could provide an in-depth and comparative understanding of the effects of different metabolites and DSMs on microbial structures. Thus, the aim of this study was to examine fungal and bacterial community structures of Arabidopsis mutants impaired in GLS, FLV and the DSMs SA, JA, ABA, ET and fatty acid biosynthesis. For comparison, we included the reference wild types used originally as backgrounds for generating the mutants.

Materials and methods

Plant material

We used 21 Arabidopsis mutants and their genetic background lines Col-0 and Ler-0 (**Additional file 1: Table S1**). The GLS (cyp79B2 and cyp79B3), FLVs (tt3, tt5) and jasmonic acid (dde2) mutants were kindly provided by Profs. Judith Bender (Brown University), Wendy Peer (University of Maryland) and Paul Staswich (University of Nebraska), respectively. The FLV mutants used in this study had a defective proanthocyanidin accumulation resulting in a transparent testa (tt) phenotype characterized by a yellowish or pale brown colour (29). Other Arabidopsis lines were supplied by the Nottingham Arabidopsis Stock Centre (NASC), UK.

Experimental design

Arabidopsis seeds were sown in pots (8cm x 8cm x 6cm) with moistened field soils collected from a fallow field (Jyndevad Research station, Denmark). Each pot represents a biological replicate of individual genotypes and replicated 5 times for all genotypes. Seeds were stratified and pots completely randomized and maintained in a greenhouse under 2017 summer conditions (**Additional file 1: Figure S1B**). Seedlings were maintained by capillary watering and regular weed removal. Sampling was done after 4 weeks of plant growth where roots were harvested and the adhering soils gently shaken off. Roots and remaining attached soil were pooled and placed into 2 ml collection tubes, frozen in liquid nitrogen and later stored in -20 °C freezers. Subsequently, the samples were lyophilized and ground using a Geno/Grinder 2010 at a rate of 1500 rpm with sterile metal balls (size 2.88mm, 3x per sample) before DNA extraction. For detailed experimental procedure, see supplementary methods and Figure S1 (**Additional file 1**).

Sample processing, sequence analysis and statistics

Sample DNA extraction and library preparation were essentially as previously described (23). Briefly, we extracted DNA using the PowerLyzer™ Power Soil® DNA Isolation Kit (Mo Bio Laboratories, Carlsbad, CA, USA). The bacterial primers S-D-Bact-0341-b-S-17, 5´-CCTACGGGNGGCWGCAG-3´ and S-D-Bact-0785-a-A-21, 5´-GACTACHVGGGTATCTAATCC-3´ (30) and the fungal primers fITS7, 5´-GTGARTCATCGAATCTTTG-3´ and ITS4, 5´-TCCTCCGCTTATTGATATGC-3´ (31) were used to amplify the V3/V4 region of the bacterial 16S rRNA and the fungal internal transcribed spacer 2 (ITS2) region, respectively. A dual indexing strategy was used and PCR conditions were as described (23). For details, see supplementary methods (**Additional file 1**). Samples were sequenced using the Illumina MiSeq platform at Eurofins MWG (Ebersberg, Germany). All the sequence files were deposited in the NCBI Sequence Read Archive (SRA) under the accession number PRJNA579829.

Sequence analysis for demultiplexing, chimera detection and removal, OTU picking, and OTU table creation were performed using vsearch version 2.6 (32), as described (23). Taxonomy assignment was carried out in QIIME version 1.9 (33). Downstream data exploration and visualization was performed in the R statistical package (34). Microbial community diversity estimations including alpha and beta diversities, species richness and dissimilarity were performed using the 'vegan' package (35) and phyloseq (36). A cutoff minimum of 500 reads for both bacteria and fungi, was used to remove samples with lower numbers of reads (**Additional file 1: Figure S2**). OTU tables were either transformed to relative abundance tables or rarified prior to alpha and beta diversity based calculations. To determine statistically significant differences in taxonomic profiles, we performed a multiple group analysis by comparing sequences assigned to different class level taxa (top 10) in mutants and their respective background controls (Col-0 or Ler-0) using the STAMP software v2.1.3 (37, 38). Genotypes were compared by ANOVA, followed by the Tukey–Kramer *post hoc* test ($p <$

0.05) using the Benjamini and Hochberg (BH) FDR for multiple comparisons. Taxa with small effect sizes were removed by filtering (effect size = 0.8). Beta diversity based PERMANOVA for partitioning of variance was calculated using UniFrac weighted matrices for bacterial communities and Bray Curtis for fungal communities using the 'adonis' test. Adonis test was performed using genotypes with at least 3 replicates. Differential OTU analysis was performed using DESeq2 (version1.22.2) (39). Datasets partitioned for each mutant and reference control were subjected to differential analysis to determine the most differentially significant bacterial and fungal taxa.

Results

We studied microbiome composition in Arabidopsis plants carrying mutations in specific steps of GLS, FLV and defense signaling pathways (**Additional file 1: Figures S3A- S3C and Table S1**). To determine genotypic effects on bacterial and fungi community structures, we split the data for mutants and their background controls into these three groups.

Species abundance differs between mutants and wild types

Bacterial and fungal relative abundances were distinct in the GLS mutants and their wild type Col-0 (**Additional file 1: Figures S4A, S4B**). We found significant differences in the mean abundance of reads belonging to Actinobacteria, Thermoleophilia and Verrucomicrobiae. The comparison between the mutants cyp79B3, cyp79B2cyp79B3 and TU3, and the reference Col-0 showed the highest differences in mean proportions of reads in the respective taxa ($p<0.001$) (**Fig. 1A**). For fungi, Sordariomycetes was highly abundant across several mutants but also in Col-0, while Eurotiomycetes was enriched in mutants compared to Col-0 (**Additional file 1: Figure S4B**). By performing ANOVA and *post hoc* Tukey's test, we found significant differences in reads assigned to Eurotiomycetes (cyp79B3 and TU3: Col-0), Olpidiomycetes (pad2_1: Col-0) and Sordariomycetes (cyp79B3 and cyp79B2cyp79B3: Col-0 and gsm1-1: Col-0) **(Fig. 1A).**

Class-level plots of bacterial and fungal relative abundances showed distinct microbial abundances in the FLV mutants and their controls (**Additional file 1**: **Figures S4C- S4D).** Multiple group analysis revealed significant differences of bacterial class assigned reads, with the strongest differences observed in Actinobacteria (Col-01:pap1-D), Phycisphaerae (Ler-0:tt7-7,), and Verrucomicrobiae (Ler-0:tt7-7, Ler-0:tt5 (**Fig. 1B**). The multiple test statistics for mean class level taxa comparison indicated significant differences in the mean of reads belonging to Eurotiomycetes (pap1-D:Col-0), Sordariomycetes (Col-0: pap1-D) and Tremellomycetes (Col-0: pap1-D) (**Fig. 1B**).

We detected shifts in the relative abundances of both bacteria and fungi at class-level in the defense signaling mutants (**Additional file 1: Figures S4E- S4F**). The bacterial class Verrucomicrobiae was the most significantly affected taxon detected in a comparison between Ler-0 and aba3-2. Reads belonging to Alphaproteobacteria and Thermoleophilia were also significantly different, respectively in the aba3-2: Ler-0 and Col-0: npr1-2 comparison (**Fig. 1C**)**.** For fungi, Sordariomycetes was significantly different between aba3-2 and Ler-0. In addition, we found significant differences in Olpidiomycetes abundance between Col-0 and pad3-1 and for Saccharomycetes between Ler-0 and aba3-2 (**Fig. 1C**).

Next, we performed differential analysis to determine microbial taxa that were significantly different between mutants and controls. A number of significantly enriched bacterial and fungal OTUs (bOTUs and fOTUs, respectively) were detected in mutants in comparison with their respective controls. For GLS, the highest numbers of differentially abundant bOTUs were observed in TU3 and cyp79B3 (**Fig. 2A, Table S2**). bOTUs representing the genera *Azospirillum* and *Fluviicola* showed the highest enrichment in several GLS mutants. Other significantly enriched genera included *Nocardioides* and *Streptomyces* in mutants such as TU3, myb51 and cyp79B3. In addition, both *Massilia* and *Flavobacterium* were significantly enriched in cyp79B3 and TU3. fOTUs assigned to the genera *Sporobolomyces* and *Emericellopsis* were the most significantly enriched cyp79B3,

184 cyp79B2cyp79B3 and TU3 GLS mutants (**Fig. 2A, Table S3**). The genus *Falciphora* was enriched
185 in both cyp79B3 and cyp79B2cyp79B3. fOTUs belonging to *Metarhizium*, *Acremonium* and
186 *Cyphellophora* were enriched in cyp79B3, while *Tetragoniomyces* and an unidentified genus in the
187 family *Pyronemataceae* were enriched in the double mutant cyp79B2 cyp79B3 (**Fig. 2A, Table S3**).
188 In addition, the genera *Clonostachys* and *Trichoderma* were enriched in TU3 and pad2-1,
189 respectively, while *Fusarium* was enriched in pen3-1-NahG.

190 In the FLV dataset, we found fewer differentially abundant bacterial genera (**Fig. 2B, Table S4**).
191 bOTUs belonging to *Flavobacterium* were generally enriched in the FLV mutants, and
192 *Rhodanobacter* and *Azospirillum* were significantly enriched in tt7-7 and pap1-D, respectively. For
193 fungi, we observed enriched genera including *Alternaria* in tt5, *Sporobolomycetes* and *Emericellopsis*
194 in pap1-D and *Cladosporium* and *Psathyrella,* and an unidentified member of the class
195 Agaricomycetes in tt7-7 (**Fig. 2B, Table S4**). Both tt7-7 and tt5 had an increased abundance of
196 *Apiotrichum*. In tt3, *Apodus* and an unidentified member of the class Leotiomycetes were enriched.
197 Surprisingly, we did not detect any significant enrichment of fungi in the tt3-1tt5-1 double mutation.

198 Defense signaling mutants including dde2, etr1-3 and 35S::ERF were enriched in bOTUs assigned to
199 *Azospirillum*, *Herminiimonas*, *Fluviicola* and *Flavobacterium* (**Fig. 2C, Table S5**). Similarly, FAD
200 mutants fad3-2 and fad7-1fad8-1 were enriched in *Azospirillum* and *Fluviicola*. Comparing the ET
201 mutants and their reference, etr1-3 had a higher number of enriched OTUs compared to 35S::ERF.
202 *Streptomycetes*, *Gaiella* and *Norcardioides* were enriched in etr1-3 only. *Noviherbaspirillum* and
203 *Candidatus Udaeobacter* were enriched in ABA mutants. The fungal class *Sporobolomyces* was
204 significantly enriched in mutants dde2, fad3-2 and fad7-1fad8-1(**Fig. 2C, Table S6).** Similarly,
205 *Emericellopsis* was highly enriched in dde2, etr1-3, and npr1-2. The ethylene mutants etr1-3 and
206 35S::ERF, had increased abundances of *Saitozyma* and an unidentified member of *Pyronemataceae*.
207 The aba mutants showed an increased abundance of *Alternaria* and fad3-2 had an increased

abundance of *Tetragoniomyces*, *Solicoccozyma* and *Clonostachys*, while fad7-1fad8-1 had a higher abundance of Mortierella, Tremellomycetes and Mortierellomycetes and an unidentified member of Eurotiomycetes (**Fig. 2C, Table S6)**.

GLS mutation affect microbial composition in roots

Bacterial alpha diversity was not significantly different between GLS mutants and their controls, although the GLS mutants gsm1-1 and pad2-1 showed the lowest bacterial alpha diversities (**Fig. 3A, Additional file 1: SF 5A, 6A**). GLS affected fungal alpha diversity (observed, $P<0.05$) (**Fig. 3B, Additional file 1: SF 5B, 6B**) but an ANOVA pairwise comparison showed no marked significant differences between mutants and control. A cyp79B2 mutation showed increased fungal alpha diversities but we noticed a decrease in the other mutants; cyp79B2cyp79B3, myb51 and pad3-1 had the lowest fungal alpha diversities when compared to Col-0.

Bacterial beta diversity analysis and visualization using PCoA ordination plots showed a clear separation of GLS mutants from Col-0 (**Fig. 4A**). We observed similar distinct clustering in the fungal PCoA plots, except that the Col-0 and pen3-1-NahG clustered together (**Fig. 4A**). PERMANOVA on the microbial communities revealed significant differences in the GLS dataset (Adonis, bacteria: $R^2= 0.31$, $P< 0.001$; fungi: $R^2= 0.27$, $P< 0.001$, **Table 1**) and thus corroborated the PCoA plots. To determine community distinctiveness as shown in PCoA plots for the GLS mutants and control, we performed PERMANOVA by comparing individual mutants to their wild type. Bacterial communities were strongly affected in cyp79B3 (Adonis, $R^2= 0.51$, $P> 0.01$) and TU3 (Adonis, $R^2= 0.50$, $P> 0.01$). A similar analysis revealed minor but significant effects ($p<0.05$) of genotypes on fungal communities. Unlike bacteria, the effects of TU3 and cyp73B3 on fungal communities were comparable ($p<0.05$) to the other GLS mutants.

FLV mutants change microbial composition in roots

While we did not find significant differences in bacterial alpha diversities (**Fig. 3A, Additional file 1: SF 5A, 6A**) in the FLV dataset, fungal alpha diversity was significantly affected (observed, $P<0.05$) (**Fig. 3B, Additional file 1: SF 5B, 6B**). However, an ANOVA pairwise comparison showed no marked differences in the alpha diversities between individual mutants and controls. PCoA ordination plots showed clustering of mutants from the controls in both bacterial and fungal datasets (**Fig. 4B**), but a PERMANOVA analysis only showed significant difference in the community structures of bacteria (Adonis, $R^2= 0.36$, $P< 0.001$, **Table 1**). Further data splitting and PERMANOVA analysis on individual mutants and their respective controls revealed that the tt7-7 mutation had the strongest effect on bacterial communities (Adonis; $R^2= 0.41$, $P<0.01$). A minor but significant genotype effects was also observed in tt3 (Adonis; $R^2= 0.22$, $P<0.05$), tt5 (Adonis; $R^2= 0.30$, $P< 0.05$) and pap1-D (Adonis; $R^2= 0.37$, $P<0.05$) (**Table 1**). In addition, a minor but significant genotype effect ($P<0.05$) was detected in fungal communities for mutants and their controls, except for tt3 (**Table 1**).

Microbial composition in roots of defense signaling mutants

Microbial diversity analysis showed that alpha diversities in both bacterial and fungal communities for the signaling mutants and their controls were non-significant (**Figs. 3A, 3B; Additional file 1: SF5 and SF6**). Both bacterial and fungal beta diversities revealed a clear separation of mutants and their controls on PCoA ordination plots (**Figs. 4C**). PERMANOVA analysis indicated a significant effect of defense signaling mutations on bacterial communities ($R^2= 0.39$, $P< 0.001$ **Table 1**) but not on fungal communities. Data partitioning for individual mutants and their respective controls showed minor but significant effects of most of the defense signaling mutants and controls on fungal communities (**Table 1**).

Discussion

Advances in plant genetics have improved our understanding of functional plant genomics in the context of plant microbe-interactions. The assembly of host-specific microbiomes involves a direct or indirect effect of gene regulatory functions underlying biochemical or defense signaling processes in plants (23,27,40). Characterizing microbiomes of mutants impaired in the synthesis of specific compounds could give us insights into host genotype-microbiome relations, enabling us in the end, to manipulate microbiomes for desired outcomes. In this study, we profiled the microbiomes of a wide range of Arabidopsis mutants and determined microbial relative abundance patterns and differentially abundant microbial taxa between mutants and their background controls.

GLS have distinct effects on the host root-associated microbiome

The identification of a range of bacterial and fungal taxa affected by the different GLS mutants demonstrated that GLS has distinct effects on specific microbial groups. Mutations in genes located at the initial steps of a biosynthetic pathway generally have more pronounced effects on the host-associated microbiota (23). Similarly, we found that both cyp79B3 and TU3 that carry mutations upstream in the GLS pathway had the highest effect on bOTUs. Nonetheless, the mutants gsm1-1, cyp79B2 and the double mutant cyp79B2cyp79B3 (with total disruption in both the indolic GLS and camalexin pathways) (41,42) with gene disruptions in the initial steps of the pathway similar to TU3 and cyp79B3 did not show the same dramatic effect on bOTUS. Moreover, the disruption of cyp79B2 and cyp79B3 genes occurring in the same step of the indolic GLS pathway or the TU1 and TU3 genes of the aliphatic GLS pathway, distinctively affected microbial composition in the respective mutants carrying these mutations. Both cyp79B2 and cyp79B3 mutants are disrupted in genes known for the same function (conversion of tryptophan to indole-3-acetaldoxime) and are therefore considered functionally redundant (41). However, Brader et al. (43) showed differences in the induction of the

277 cyp79B2 and cyp79B3 genes upon treatment with culture filtrates of the bacterium *Erwinia*
278 *carotovora*. Hence, it is possible that unknown enzymatic and pleiotropic activities of the cyp79B2
279 and cyp79B3 genes contributed to the observed differences of microbial structures. Furthermore,
280 Ludwig-Müller et al. (44) reported that several TU mutants developed varying degrees of clubroot
281 disease symptoms caused by *Plasmodiophora brassicae*. In that study, different contents of GLS
282 intermediate products were found in the TU lines. Buxdorf *et al.* (45) showed that fungal pathogens,
283 such as the Brassicaceae pathogen *Alternaria brassicola,* were less sensitive to GLS when compared
284 to non-adapted fungi. Furthermore, *B. cinerea* isolates were reported to display strain-specific
285 sensitivity to GLS (46). The increased abundance of individual bacterial genera such as *Azospirillum*
286 and *Fluviicola* as well as fungal genera *Sporobolomyces* and *Emericellopsis* in several GLS mutants
287 could further confirm the "gating" role of specific metabolic profiles on individual microbial taxa
288 (23,27). Plant metabolic compounds with antimicrobial properties including GLS are known to
289 constitute the root rhizoplane's boundary layers that modulate host root microbiome assembly
290 (23,47,48). Altogether, these data confirm the GLS specific effects on microbial communities.

291 Genera such as *Azospirillum, Nocardioides* and the plant beneficial taxa *Streptomyces* and
292 *Flavobacterium* were affected in some of the GLS mutants. Also, *Azospirillum* contains several
293 beneficial species, widely known for their plant growth promoting traits including nitrogen fixation
294 and the synthesis of phytohormones and other compounds required for both biotic and abiotic
295 tolerance (49). In particular, the upstream mutations cyp79B3 and TU3 mutants were highly enriched
296 in *Flavobacterium* and *Massilia.* The yeasts *Sporobolomyces,* which were enriched mostly in the
297 FAD, dde2 and npr1-2 mutants, are abundant members of the plant mycobiome (50,51) and have
298 been shown to have antagonistic effects against pathogens (52). Some members of *Emericellopsis* are
299 known to possess biocontrol traits via the antimicrobial compound emericellipsin A, which have been
300 shown to suppress the pathogen *Aspergillus niger* (53).

Furthermore, the clear separation of GLS mutants from Col-0 observed on a PCoA plot further supports our findings. In particular, the bacterial communities were strongly affected in cyp79B3 and TU3 mutants. Similarly, Micallef and Colón-Carmona (54) showed that overexpressed Arabidopsis mutants atr1D (with elevated GLS levels) and the double mutant cyp79B2cyp79B3 had distinct rhizobacterial community structures. Bressan et al. (21) also showed distinct differences in microbial community composition of the GLS mutant cyp79A1 and the control Col-0. Together, these findings confirm our hypothesis of the effect of gene mutations in metabolic pathways on the innate plant recruitment potential.

Flavonoid affect the host root-associated microbiomes

By comparing the microbiomes of FLV mutants and controls, we observed distinct effects on microbial composition. In addition, significant differences between mutants and the controls were observed at higher taxonomic ranks including Actinobacteria, Thermoleophilia and Verrucomicrobiae as well as the fungal classes Sordariomycetes and Eurotiomycetes. Previously, it has been shown that FLVs affects microbial community structures (55) while other studies have reported non-significant effects of some FLV mutations on microbial community structures (20). Surprisingly, while mutations in single genes (in tt3 and tt5) significantly affected both bacterial and fungal communities, the double mutant tt3-1tt5-1 only had significant effects on fungal communities. Associated pleiotropic effects of the mutations resulting in unpredictable FLV profiles (56,57) could explain this observation.

Arabidopsis predominantly produce the flavonols, kaempferol and quercetin glycosides (58). The observed effect of the tt7-7 mutation in the present study suggests a more pronounced effect of the depletion of both quercetin and kaempferol on bacterial communities. Gene disruptions in the tt mutants have been shown to accumulate varying FLV profiles (14,8,59,60). For example, the tt3

mutant with disruption in the dihydroflavonol 4-reductase gene located downstream in the FLV biosynthetic pathway was shown to accumulate appreciate levels of the intermediate products quercetin and kaempferol (14). The tt5 with a disruption in the chalcone-flavanone isomerase gene was reported to lack flavonols but had detectable levels of the intermediates naringenin chalcone, chalcone and flavanone (14). Kaempferol and naringenin inhibits spore germination of plant pathogens (61) while quercetin enhances mycorrhizal-plant symbiosis by stimulating host penetration and hyphal growth (7). The biocontrol activity of the isoflavonoid flavans and flavanones (16) extend to their ability to modulate genes regulating the synthesis of the antifungal compound 2,4-diacetylphloroglucinol and pyoluteorin by the biocontrol agent *Pseudomonas fluorescens* CHA0 (62). In addition, Vandeputte *et al.* (61,62) demonstrated naringenin and catechin produced in higher plants to be important in reducing the production of quorum sensing-controlled virulence factors in *Pseudomonas aeruginosa* PAO1. The fact that we only observed few differentially abundant bacterial taxa when compared to fungi suggests a stronger effect of FLVs on fungi. The observed differential effect of FLVs on fungal taxa corroborates the finding of distinct effects of FLVs on individual fungi such as arbuscular mycorrhizal fungi (63). The strong enrichment of the plant pathogenic genus *Alternaria* in tt5 mutants indicates that naringenin could play a defensive role against plant pathogens, as suggested previously (62). In summary, like the GLS, FLVs could have a strong innate microbial recruitment role and are thus important for the modulation of root-associated microbiomes.

Defense signaling mutations affect host root-microbiome assembly.

Similar to the GLS and FLV mutations, DSMs strongly affected microbial communities with specific effects of individual mutants on both bacterial and fungal communities. The observed differential effects of both ET insensitive and overexpressed mutants on microbial communities confirm previous studies (64,65). The detection of ABA mutation affecting microbial taxa, for example, the enrichment of Acidobacteria, Alphaproteobacteria and Sordariomycetes taxa in aba mutant compared to Ler-0

348 support that ABA preferentially affect Arabidopsis-root associated microbiota (66). Studies have
349 shown that ABA is a key regulator of defense and in many instances was found to suppress the
350 activation of plant defense genes (67,68,69). While the mechanism of negative defense modulation
351 activity of ABA is not well understood, we speculate that ABA depletion of core microbial taxa in
352 Arabidopsis, Alphaproteobacteria and Sordariomycetes (70,71), detected in Ler-0 in this study could
353 contribute to the weak defense against pathogens.

354 FAD is pivotal in the hormonal signaling network by modulating both the SA (72) and JA pathways
355 (73), and its role in mediating plant-microbe interactions has been reported (19,28). Our study
356 revealed distinct differential effect of FAD mutants on microbial community structures but both
357 mutants revealed increased enrichment of the bacterial genera *Azospirillum* and fungal
358 *Sporobolomyces* (for fad7-1fad8-1) or unidentified genus in the Sporidiobolaceae (for fad3-2). This
359 finding corroborates a previous study where the Arabidopsis triple mutant fad3fad7fad8 had higher
360 bacterial diversity compared to the control, with several species within Alpha- and
361 Gammaproteobacteria enriched in the FAD mutant (28). Moreover, differential effects of FAD genes
362 on specific microbial members have been reported. For instance, while the FAD3 gene was shown to
363 be unresponsive upon inoculation of the bacterial pathogen *Xanthomonas campestris* (72), FAD7
364 genes are known to be induced by fungal effectors (74). The observation of differential effects of
365 FAD single or double mutations on microbial communities indicate specific effects of individual
366 FAD genes on the host associated microbiomes. However, hormonal crosstalk mechanisms could be
367 involved in the observed effects of FAD mutation on microbial communities.

368 In addition, the observed strongest effect of ABA and the FAD double mutant on bacterial
369 communities (PERMANOVA, 39% and 46%) could further suggest a higher pronounced modulating
370 role of these molecules on bacterial community assembly. The JA mutant dde2 significantly affected
371 both bacterial and fungal communities. This finding corroborates a study in which JA mutants myc2

and med25 were reported to sculpt distinct bacterial and archaeal compositions when compared to the control (64). In general, we have demonstrated that mutations in signaling pathways affect microbial community structures, while differentially affected microbial taxa further supports this. These results are consistent with previous findings (27), however, the inclusion of a range of mutants in different signaling pathways in the present study has expanded on the scope of the subject.

A cascading effect of immune system activation is the induction of systemic acquired resistance (SAR) and induced systemic resistance (ISR), with the phytohormones SA, JA, ABA and ET acting as DSMs (9). Hormonal cross-talk mechanisms implicate the interaction of these signaling hormones in fine-tuning defense against biotic and abiotic stresses (9, 75). For example, ABA is reported to be involved in SA-JA-ET networks, and therefore important in subsequent defense activations (9,76–78). This interconnectedness in signaling pathways presents a high complexity, thus, mutant lines with several mutations with the possible elimination of overlapping defense-signaling functions are highly recommended (27). Pleiotropic effects arising, for instance, from a disruption in the NPR1 gene makes it impossible to examine the exact effect of SA on microbial community structures. As such, it is difficult to make definitive conclusions with the specific mutations on microbial communities. We therefore suggest that a detailed analysis could include mutants with complete abolishment of interactive pathways, complemented with other omics analysis techniques.

Conclusions

Plant metabolic and defense signaling pathways are an integral part of the innate sculpting mechanisms that regulate the assembly of host-associated microbiota. By using different Arabidopsis mutants and their background controls, we showed that both secondary metabolism and DSMs affect bacterial and fungal community structures. We found the bacterial taxa Actinobacteria, Thermoleophilia and Verrucomicrobiae and the fungal taxa Eurotiomycetes, Olpidiomycetes and

Sordariomycetes to be the most highly affected between mutants and their controls. Differential analysis at lower taxonomic levels revealed significantly affected genera between Arabidopsis GLS, FLVs and defense signaling mutants and their respective controls. These results strongly support the perception that many plant secondary metabolites and DSMs affect microbiome assembly. Our findings suggest that disruption of secondary metabolite or signaling pathways affect the innate mechanisms that modulate root-associated microbiome assembly. Further analysis complemented by other omics techniques could provide an indepth understanding of the plant-omics links, thus facilitating the utilization of microbiome solutions for sustainable plant production.

Acknowledgements

We thank Profs Judith Bender (Brown University, USA), Wendy Peer (University of Maryland, USA) and Paul E. Staswich (University of Nebraska, USA) for kindly providing the Arabidopsis mutants. We thank Simone Ena Rasmussen and Mathilde Schiøtt Dige for their excellent laboratory technical assistance.

Funding

This work was financially supported by Aarhus University (project number 22550) and the Independent Research Fund Denmark (DFF), grant number 6111-00065B.

Availability of data and materials

The MiSeq paired end reads for bacterial 16 s rRNA gene (V3-V4) and fungal ITS2 regions have been deposited in the NCBI Sequence Read Archive (SRA) database under the accession number PRJNA579829.

Authors' contributions

ENK, RS and MN conceived the study, participated in its design, and wrote the paper. ENK and RS conducted the experiment and analyzed the data. All authors read and approved the manuscript.

Ethics approval and consent to participate

Not applicable.

Competing interests

The authors declare that they have no conflict of interest.

List of Tables

Table 1. Permutation analysis of variance (PERMANOVA) for individual mutants and background controls. Adonis tests were based on weighted UniFrac matrices for bacterial and Bray-Curtis distance matrices for fungal community dissimilarity assessment using 1000 permutations.

Dataset/ Factor	**Genotype description**	**Bacteria (R^2)**	**Fungi (R^2)**
GLS (Mut1)	GLS mutants and wild type	0.31***	0.27***
FLV (Mut2)	FLV mutants and wild types	0.36***	--
DSM (Mut3)	Defense signaling mutants and wild types	0.39***	--
GLS			
Col-0_*cyp79B3*	IGS partial disruption)	0.51**	--
Col-0_*cyp79B2cyp79B3*	Lacks IGS and camalexin (Blocked in the production of I3AOx))	0.43*	0.31*
Col-0_*myb51*	IGS synthesis disruption	0.36*	0.24*
Col-0_*gsm1-1*	Reduced amounts of many aliphatic glucosinolates	0.33*	0.30*

Col-0_*TU3*	Deficient in aliphatic GLS with heptyl and octyl core groups	0.50**	0.37*
Col-0_ *pad2-1*	Partially blocks camalexin	--	0.38*
Col-0_ pen3-1-NahG	Disruption in both IGS synthesis and SA signaling pathways.	0.27*	--
FLV			
Ler-0_tt7-7	Deficient in flavonoid 3'-hydroxylase activity and lacks orthodihydroxy flavonoids such as quercetin and kaempferol	0.41**	0.22*
Ler-0_tt3	Excess quercetin, kaempferol	0.22*	--
Ler-0_tt5	Low-level quercetin production	0.30*	0.25*
Ler-0_ tt3-1tt5-1	Double mutation, disruption of the synthesis of brown pigment	--	0.16*
Col-0_pap1-D	Overexpressed (anthocyanin) mutant	0.37*	0.30*
DSMs			
Col-0_*dde2*	JA deficient	0.33*	0.34*
Ler-0_ *aba3-2*	ABA deficient	0.39**	0.30*
Col-0_ *etr1-3*	Ethylene responsive	0.47*	0.31*
Col-0_*35S::ERF*	Ethylene (overexpressed)	0.32*	0.24*
Col-0_ *fad3-2*	Fatty acid desaturase (FAD) deficient	--	0.18*
Col-0_ *fad7-1fad8-1*	FAD double mutation	0.46**	--

Significance of test indicated as *** for $p<0.001$, ** $p>0.01$, *$p<0.05$ and R^2 for the proportion of variation explained. I3AOx (Indole-3-aldoxime) IGS (indole glucosinolate)

List of figures

Figure 1. Bar plots showing mean distribution of reads assigned at class level in **A**) GLS mutants and their controls, **B**) FLV mutants and their controls and **C**) defense signaling mutants and their controls. Mutants were compared to their background controls by ANOVA, followed by the Tukey–Kramer *post hoc* test ($p < 0.05$) using the Benjamini and Hochberg (BH) FDR for multiple comparisons. Only top 10 taxa were used and taxa with small effect sizes were removed by filtering (effect size = 0.8).. The black and white bar plots represent controls and mutants respectively. Error bars represent standard deviations. The analysis was performed using the STAMP software (v2.1.3)

Figure 2: Network showing microbial differential analysis between mutants and controls. Bacterial and fungal genera that were significantly affected are shown for **A**) GLS mutants and control. **B**) FLV mutants and control **C**) defense signaling mutants and control. Analysis performed using DESeq2. Enrichment in mutants are shown in red and in blue for controls. Line width indicates the significant level of effect.

Figure 3. Alpha diversity estimated using Shannon diversity for the respective genotypes.
A) Bacterial and (**B**) fungal Shannon diversity in different genotypes. Samples with at least 3 replicates for both bacteria and fungi (with bacterial and fungal reads >800 and >500 respectively) are shown.

Figure 4. Principal coordinate analysis (PCoA) of weighted UniFrac distances (bacterial) and Bray-Curtis (fungal) between GLS (**A**), FLV (**B**) and DSM (**C**) genotypes. Individual genotypes and sample groups are shown in different colours and shapes.

Additional file 1

Supplementary figures

Figure S1. Arabidopsis growth and harvesting scheme. A) Arabidopsis growing under greenhouse conditions. B) Summer conditions (temperature and relative humidity (RH) for the growth of Arabidopsis in greenhouses. Each bar represent daily readings (at hourly intervals) Weather data was obtained from the DMI Dalmose station. C) Arabidopsis with the roots (circled in red), the part harvested for analysis D) Root samples from individual plants in same pots were pooled into in a collection tube (representing a replicate) and subsequently frozen.

Figure S2. Schematics of biosynthetic and signaling pathways. A) Biosynthetic pathway of aliphatic and indolic GLS in Arabidopsis. Schematic overview of genes involved at the different steps of the pathway. Disrupted genes from which mutants were derived are in bold while mutants are shown in blue. Adapted from suppl. ref: 1, 2, 3, 4 and 5. IAN (Indole-3-acetonitrile), TSB1 (tryptophan synthase beta subunit 1). B) The FLV biosynthetic pathway. The transparent testa (tt) mutations in mutants (parentheses) used in this study are indicated. Enzyme abbreviations: CHI, chalcone isomerase; CHS, chalcone synthase; DFR, dihydroflavonol reductase; F3H, flavonol 3-hydroxylase; FLS, flavonol synthase. *(double mutant). Adapted from suppl ref. 6. C) The schematics of signaling pathways. The phytohormones salicylic acid (SA), jasmonic acid (JA), ethylene (ET), abscisic acid (ABA) mediate defense signaling in plants. Fatty acid desaturase (FAD) is also involved in defense including the regulation of JA and SA pathways. Genes of interest (bold) in a pathway and mutants (blue) carrying a mutation in these genes are represented. Defense cross-talk interactions that fine-tune defense signaling outcomes is also shown. NPR1 (Non-expressor of PR genes1), AAO3 (Abscisic acid synthase), AOS (Allene oxide synthase).

Figure S3. Box plots showing the distribution of the number of reads and OTU distribution in each sample used in this study. A) Bacterial reads and B) OTU distribution, C) fungal reads and D) OTU distribution.

Figure S4. Class-level relative abundances of microbial communities Arabidopsis genotypes. a) Bacterial relative abundance at class level in the different GLS mutants and controls, Col-0. b). Bacterial relative abundance at class level in the different GLS mutants and controls, Col-0. c). Bacterial relative abundance at class level in the different plant FLV mutants and controls, Col-0 and Ler-0. d) Fungal relative abundance at class level in the different FLV mutants and controls, Col-0 and Ler-0. e) Bacterial relative abundance at class level in the different defense signaling mutants and controls, Col-0 and Ler-0. f) Fungal relative abundance at class level in the different defense signaling mutants and controls, Col-0 and Ler-0.

Figure S5. Observed bacterial (A) and fungal (B) OTU richness in the different genotypes. Samples with at least three replicates (with bacterial and fungal reads >800 and >500 respectively) are shown.

Figure S6. Alpha diversities estimated in the respective genotypes using observed OTU richness and Shannon diversity matrices for A) Bacteria and B) Fungi. All sample with reads >800 for bacterial and >500 fungal are presented.

Supplementary tables

Table S1. List of Arabidopsis genotypes used for the study.

Table S1. Differentially abundant bacterial OTUs on roots of Col-0 and GLS mutants as determined using DESeq2.

Table S2. Differentially abundant fungal OTUs on roots of Col-0 and GLS mutants; as determined using DESeq2.

Table S3. Differentially abundant bacterial OTUs on roots of Ler-0 or Col-0 and FLV mutants as determined using DESeq2.

Table S4. Differentially abundant fungal OTUs on roots of Ler-0 or Col-0 and FLV mutants as determined using DESeq2.

Table S5. Differentially abundant bacterial OTUs on roots of Col-0 or Ler-0 and signaling mutants as determined using DESeq2.

Table S6. Differentially abundant fungal OTUs on roots of Col-0 or Ler-0 and signaling mutants as determined using DESeq2.

References

1. Chisholm ST, Coaker G, Day B, Staskawicz BJ. Host-microbe interactions: shaping the evolution of the plant immune response. Cell. 2006;124(4):803–14.

2. Jones JDG, Dangl L. The plant immune system. Nature. 2006; 444:323–9.

3. Kliebenstein DJ. Secondary metabolites and plant/environment interactions: A view through *Arabidopsis thaliana* tinged glasses. Plant, Cell Environ. 2004;27(6):675–84.

4. Kirkegaard JA, Sarwar M. Biofumigation potential of brassicas I. Variation in glucosinolate

519 profiles of diverse field-grown brassicas. 1998;71–89.

520 5. Tierens KF, Thomma BP, Brouwer M, Schmidt J, Kistner K, Porzel a, et al. Study of the role
521 of antimicrobial glucosinolate-derived isothiocyanates in resistance of Arabidopsis to microbial
522 pathogens. Plant Physiol. 2001;125:1688–99.

523 6. Angus JF, Gardner PA, Kirkegaard JA, Desmarchelier JM. Biofumigation: Isothiocyanates
524 released from brassica roots inhibit growth of the take-all fungus. Plant Soil. 1994;162:107–12.

525 7. Cesco S, Mimmo T, Tonon G, Tomasi N, Pinton R, Terzano R, et al. Plant-borne flavonoids
526 released into the rhizosphere: Impact on soil bio-activities related to plant nutrition. A review.
527 Biol Fertil Soils. 2012;48(2):123–49.

528 8. Buer CS, Imin N, Djordjevic MA. Flavonoids: New roles for old molecules. J Integr Plant
529 Biol. 2010;52: 98–111.

530 9. Pieterse CMJ, Leon-Reyes A, Van Der Ent S, Van Wees SCM. Networking by small-molecule
531 hormones in plant immunity. Nat Chem Biol. 2009;5(5):308–16.

532 10. Hacquard S, Spaepen S, Garrido-Oter R, Schulze-Lefert P. Interplay between innate immunity
533 and the plant microbiota. Annu Rev Phytopathol. 2017;55(1):565–89.

534 11 Graser G, Oldham NJ, Brown PD, Temp U, Gershenzon J. The biosynthesis of benzoic acid
535 glucosinolate esters in *Arabidopsis thaliana*. Phytochemistry. 2001;57(1):23–32.

536 12. Halkier BA, Gershenzon J. Biology and biochemistry of glucosinolates. Annu Rev Plant Biol.
537 2006;57:303–33.

538 13. Haughn GW, Davin L, Giblin M, Underhill EW. Biochemical genetics of plant secondary
539 metabolites in *Arabidopsis thaliana*. Plant Physiol.1991;217–26.

14. Peer WA, Brown DE, Tague BW, Muday GK, Taiz L, Murphy AS. Flavonoid accumulation patterns of transparent testa mutants of Arabidopsis. Plant Physiol. 2001;126(2):536–48.

15. Saito K, Yonekura-Sakakibara K, Nakabayashi R, Higashi Y, Yamazaki M, Tohge T, et al. The flavonoid biosynthetic pathway in Arabidopsis: Structural and genetic diversity. Plant Physiol Biochem. 2013;72:21–34.

16. Weston LA, Mathesius U. Flavonoids: their structure, biosynthesis and role in the rhizosphere, including allelopathy. J Chem Ecol. 2013;39(2):283–97.

17. Staswick PE, Yuen GY, Lehman CC. Jasmonate signaling mutants of Arabidopsis are susceptible to the soil fungus *Pythium irregulare*. Plant J. 1998;15(6):747–54.

18. Soliman S, El-Keblawy A, Mosa KA, Helmy M, Wani SH. Understanding the phytohormones biosynthetic pathways for developing engineered environmental stress-tolerant crops. Biotechnologies of crop improvement, Volume 2: Transgenic Approaches. 2018: 1–485.

19. Kachroo P, Shanklin J, Shah J, Whittle EJ, Klessig DF. A fatty acid desaturase modulates the activation of defense signaling pathways in plants. Proc Natl Acad Sci. 2002;98(16):9448–53.

20. Badri D V., Quintana N, El Kassis EG, Kim HK, Choi YH, Sugiyama A, et al. An ABC transporter mutation alters root exudation of phytochemicals that provoke an overhaul of natural soil microbiota. Plant Physiol. 2009;151(4):2006–17.

21. Bressan M, Achouak W, Berge O. Exogenous glucosinolate produced by transgenic *Arabidopsis thaliana* has an impact on microbes in the rhizosphere and plant roots. ISME J. 2009;3:1243–57.

22. Hu L, Robert CAM, Cadot S, Zhang X, Ye M, Li B, et al. Root exudate metabolites drive

plant-soil feedbacks on growth and defense by shaping the rhizosphere microbiota. Nat Commun. 2018;9(1):1–13.

23. Kudjordjie EN, Sapkota R, Steffensen SK, Fomsgaard IS, Nicolaisen M. Maize synthesized benzoxazinoids affect the host associated microbiome. Microbiome. 2019;1–17.

24. Stringlis IA, Yu K, Feussner K, de Jonge R, Van Bentum S, Van Verk MC, et al. MYB72-dependent coumarin exudation shapes root microbiome assembly to promote plant health. Proc Natl Acad Sci. 2018; 115(22): 5213-5222.

25. Lundberg DS, Teixeira PJPL. Root-exuded coumarin shapes the root microbiome. Proc Natl Acad Sci. 2018;115 (22): 5629-5631.

26. Voges MJEEE, Bai Y, Schulze-Lefert P, Sattely ES. Plant-derived coumarins shape the composition of an Arabidopsis synthetic root microbiome. Proc Natl Acad Sci. 2019;116(25):12558–12565.

27. Lebeis SL, Paredes SH, Lundberg DS, Breakfield N, Gehring J, McDonald M, et al. Salicylic acid modulates colonization of the root microbiome by specific bacterial taxa. Science. 2015;349(6250):860–4.

28. Kniskern JM, Traw MB, Bergelson J. Salicylic acid and jasmonic acid signaling defense pathways reduce natural bacterial diversity on *Arabidopsis thaliana*. Mol Plant Microbe Interact. 2007;20(12):1512–22.

29. Shirley BW, Kubasek WL, Storz G, Bruggemann E, Koornneef M, Ausubel FM, et al. Analysis of Arabidopsis mutants deficient in flavonoid biosynthesis. Vol. 8, The Plant journal. 1995. 659–71.

582 30. Ihrmark K, Bödeker ITM, Cruz-Martinez K, Friberg H, Kubartova A, Schenck J, *et al.* New
583 primers to amplify the fungal ITS2 region - evaluation by 454-sequencing of artificial and
584 natural communities. FEMS Microbiol Ecol . 2012;82: 666–677.

585 31. Klindworth A, Pruesse E, Schweer T, Peplies J, Quast C, Horn M, et al. Evaluation of general
586 16S ribosomal RNA gene PCR primers for classical and next-generation sequencing-based
587 diversity studies. Nucleic Acids Res. 2013;41(1):e1.

588 32. Rognes T, Flouri T, Nichols B, Quince C, Mahé F. VSEARCH: a versatile open source tool
589 for metagenomics. PeerJ. 2016;4:e2584.

590 33. Caporaso JG, Kuczynski J, Stombaugh J, Bittinger K, Bushman FD, Costello EK, et al. QIIME
591 allows analysis of high-throughput community sequencing data. Nat Methods. 2010;7(5):335–
592 6.

593 34. R Core Team. R : A language and environment for statistical computing. 2017:(2).

594 35. Oksanen AJ, Blanchet FG, Friendly M, Kindt R, Legendre P, Mcglinn D, et al. Vegan:
595 Community ecology package. 2019. Version 2.5-6.

596 36. McMurdie PJ, Holmes S, Kindt R, Legendre P, O'Hara R. phyloseq: An R package for
597 reproducible interactive analysis and graphics of microbiome census data. PLoS One.
598 2013;8(4):e61217.

599 37. Parks DH, Tyson GW, Hugenholtz P, Beiko RG. STAMP: statistical analysis of taxonomic
600 and functional profiles. Bioinformatics. 2014;30:3123-3124.

601 38. Parks DH and Beiko RG. Identifying biologically relevant differences between metagenomic
602 communities. Bioinformatics. 2010;26:715-721.

603 39. Love MI, Huber W, Anders S. Moderated estimation of fold change and dispersion for RNA-
604 seq data with DESeq2. Genome Biol. 2014;15(12):1–21.

605 40. Zhalnina K, Louie KB, Hao Z, Mansoori N, Da Rocha UN, Shi S, et al. Dynamic root exudate
606 chemistry and microbial substrate preferences drive patterns in rhizosphere microbial
607 community assembly. Nat Microbiol. 2018;3(4):470–80.

608 41. Zhao Y, Hull AK, Ecker JR, Normanly J, Chory J, Celenza JL. Trp-dependent auxin
609 biosynthesis in. Genes Dev. 2002;3:100–12.

610 42. Glawischnig E. Camalexin. Phytochemistry. 2007;68(4):401–6.

611 43. Brader G, Tas E, Palva ET. Jasmonate-dependent induction of indole glucosinolates in
612 Arabidopsis by culture filtrates of the nonspecific pathogen *Erwinia carotovora*. Plant Physiol.
613 2001;126(2):849–60.

614 44. Ludwig-Müller J, Pieper K, Ruppel M, Cohen JD, Epstein E, Kiddle G, et al. Indole
615 glucosinolate and auxin biosynthesis in *Arabidopsis thaliana* (L.) Heynh. glucosinolate
616 mutants and the development of clubroot disease. Planta. 1999;208(3):409–19.

617 45. Buxdorf K, Yaffe H, Barda O, Levy M. The effects of glucosinolates and their breakdown
618 products on necrotrophic fungi. PLoS One. 2013;8(8).

619 46. Kliebenstein DJ, Rowe HC, Denby KJ. Secondary metabolites influence Arabidopsis/Botrytis
620 interactions: Variation in host production and pathogen sensitivity. Plant J. 2005;44(1):25–36.

621 47. Reinhold-Hurek B, Bünger W, Burbano CS, Sabale M, Hurek T. Roots shaping sheir
622 microbiome: Global hotspots for microbial activity. Annu Rev Phytopathol. 2015;53(1):403–
623 24.

624 48. van der Heijden MGA, Schlaeppi K. Root surface as a frontier for plant microbiome research:
625 Fig. 1. Proc Natl Acad Sci. 2015;112(8):2299–300.

626 49. Fukami J, Cerezini P, Hungria M. *Azospirillum*: benefits that go far beyond biological nitrogen
627 fixation. AMB Express. 2018;8(1):1–12.

628 50. Sapkota R, Jørgensen LN, Nicolaisen M. Spatiotemporal variation and networks in the
629 mycobiome of the wheat canopy. Front Plant Sci. 2017;8:1357.

630 51. Sapkota R, Knorr K, Jørgensen LN, Hanlon K a O, Nicolaisen M. Host genotype is an
631 important determinant of the cereal phyllosphere mycobiome. New Phytol. 2015;207(4):1134–
632 44.

633 52. Wachowska U, Borowska J. Antagonistic yeasts competes for iron with winter wheat stem
634 base pathogens. Gesunde Pflanz. 2014;66(4):141–8.

635 53. Rogozhin EA, Sadykova VS, Baranova AA, Vasilchenko AS, Lushpa VA, Mineev KS, et al.
636 A novel lipopeptaibol emericellipsin A with antimicrobial and antitumor activity produced by
637 the extremophilic fungus emericellopsis alkalina. Molecules. 2018;23(11).

638 54. Micallef S, Colón-Carmona A. Genetic and developmental control of rhizosphere bacterial
639 communities. Mol Microb Ecol Rhizosph. 2013;1:257–63.

640 55. Czaban W, Rasmussen J, Laursen BB, Vidkjær NH, Sapkota R, Nicolaisen M, et al. Multiple
641 effects of secondary metabolites on amino acid cycling in white clover rhizosphere. Soil Biol
642 Biochem. 2018;123.

643 56. Sugiyama A, Yazaki K. Flavonoids in plant rhizospheres: Secretion, fate and their effects on
644 biological communication. Plant Biotechnol. 2014;31(5):431–43.

645 57. Saslowsky DE, Dana CD, Winkel-shirley B. An allelic series for the chalcone synthase locus
646 in Arabidopsis. Gene. 2000;255:127–38.

647 58. Buer CS, Djordjevic MA. Architectural phenotypes in the transparent testa mutants of
648 Arabidopsis thaliana. J Exp Bot . 2009;60: 751–763.

649 59. Padmavati M, Sakthivel N, Thara K V., Reddy AR. Differential sensitivity of rice pathogens
650 to growth inhibition by flavonoids. Phytochemistry. 1997;499–502.

651 60. Werra P De, Tabacchi R, Keel C, Maurhofer M. Plant- and microbe-derived compounds affect
652 the expression of genes encoding antifungal compounds in a Pseudomonad with biocontrol
653 activity. Appl enviromental Microbiol. 2011;77(8):2807–12.

654 61. Vandeputte OM, Kiendrebeogo M, Rajaonson S, Diallo B, Mol A, Jaziri M El, et al.
655 Identification of catechin as one of the flavonoids from combretum albiflorum bark extract that
656 reduces the production of quorum-sensing-controlled virulence factors in Pseudomonas
657 aeruginosa PAQ1. Appl Environ Microbiol. 2010;76(1):243–53.

658 62. Vandeputte OM, Kiendrebeogo M, Rasamiravaka T, Stévigny C, Duez P, Rajaonson S, et al.
659 The flavanone naringenin reduces the production of quorum sensing-controlled virulence
660 factors in Pseudomonas aeruginosa PAO1. Microbiology. 2011;157(7):2120–32.

661 63. Scervino JM, Ponce MA, Erra-Bassells R, Vierheilig H, Ocampo JA, Godeas A. Flavonoids
662 exhibit fungal species and genus specific effects on the presymbiotic growth of Gigaspora and
663 Glomus. Mycol Res. 2005;109(7):789–94.

664 64. Bodenhausen N, Bortfeld-Miller M, Ackermann M, Vorholt JA (2017) A synthetic community
665 approach reveals plant genotypes affecting the phyllosphere microbiota. PLoS Genet
666 (2017);10(4): e1004283.

667 65 Doornbos RF, Geraats BPJ, Kuramae EE, Van Loon LC, Bakker P AHM. Effects of jasmonic
668 acid, ethylene, and salicylic acid signaling on the rhizosphere bacterial community of
669 *Arabidopsis thaliana*. Mol Plant Microbe Interact. 2011;24:395–407.
670

671 66. Carvalhais LC, Dennis PG, Badri D V, Kidd BN, Vivanco JM, Schenk PM. Linking jasmonic
672 acid signaling, root exudates, and rhizosphere microbiomes. Mol Plant Microbe Interact.
673 2015;28(9):1049–58.

674 67. Adie BA, Pérez-Pérez J, Pérez-Pérez MM, Godoy M, Sánchez-Serrano JJ, Schmelz EA, et al.
675 ABA is an essential signal for plant resistance to pathogens affecting JA biosynthesis and the
676 activation of defenses in Arabidopsis. Plant Cell. 2007;19(5):1665–81. 68 Xiong L, Yang Y.
677 Disease resistance and abiotic stress tolerance in rice are inversely modulated by an abscisic
678 acid–inducible mitogen-activated protein kinase. Plant Cell. 2003;15:745–59.

679 69 Gao S, Guo W, Feng W, Liu L, Song X, Chen J, et al. LTP3 contributes to disease susceptibility
680 in Arabidopsis by enhancing abscisic acid (ABA) biosynthesis. Mol Plant Pathol.
681 2016;17:412–26.
682
683 70 Hacquard Stephane, Garrido-Oter R, Anthonio G, Spaepen S, Ackermann G, Lebeis S, et al.
684 Microbiota and host nutrition across plant and animal kingdoms. 2015;603–16.

685 71 Almario J, Jeena G, Wunder J, Langen G, Zuccaro A, Coupland G, Bucher M. Root-associated
686 fungal microbiota of nonmycorrhizal *Arabis alpina* and its contribution to plant phosphorus
687 nutrition. Proc Natl Acad Sci. 2017;114:9403-12.

688 72. Buell CR, Somerville SC. Expression of defense-related and putative signaling genes during
689 tolerant and susceptible interactions of Arabidopsis with *Xanthomonas campestris pv.*

690 *campestris*. Mol Plant Microbe Interact. 1995;8: 435–43.

691 73. Kirsch C, Takamiya-Wik M, Reinold S, Hahlbrock K, Somssich IE. Rapid, transient, and
692 highly localized induction of plastidial ω-3 fatty acid desaturase mRNA at fungal infection
693 sites in *Petroselinum crispum*. Proc Natl Acad Sci. 1997;94(5):2079–84.

694 74. Avila CA, Arevalo-Soliz LM, Jia L, Navarre DA, Chen Z, Howe GA, et al. Loss of function
695 of fatty acid desaturase7 in tomato enhances basal aphid resistance in a salicylate-dependent
696 manner. Plant Physiol. 2012;158(4):2028–41.

697 75. Pieterse CMJ, Van der Does D, Zamioudis C, Leon-Reyes A, Van Wees SCM. Hormonal
698 modulation of plant immunity. Annu Rev Cell Dev Biol. 2012;28(1):489–521.

699 76. Anderson JP. Antagonistic interaction between abscisic acid and jasmonate-ethylene signaling
700 pathways modulates defense gene expression and disease resistance in Arabidopsis. Plant Cell.
701 2004;16(12):3460–79.

702 77. Flors V, Ton J, Van Doorn R, Jakab G, García-Agustín P, Mauch-Mani B. Interplay between
703 JA, SA and ABA signalling during basal and induced resistance against *Pseudomonas syringae*
704 and *Alternaria brassicicola*. Plant J. 2008;54(1):81–92.

705

706

Figures

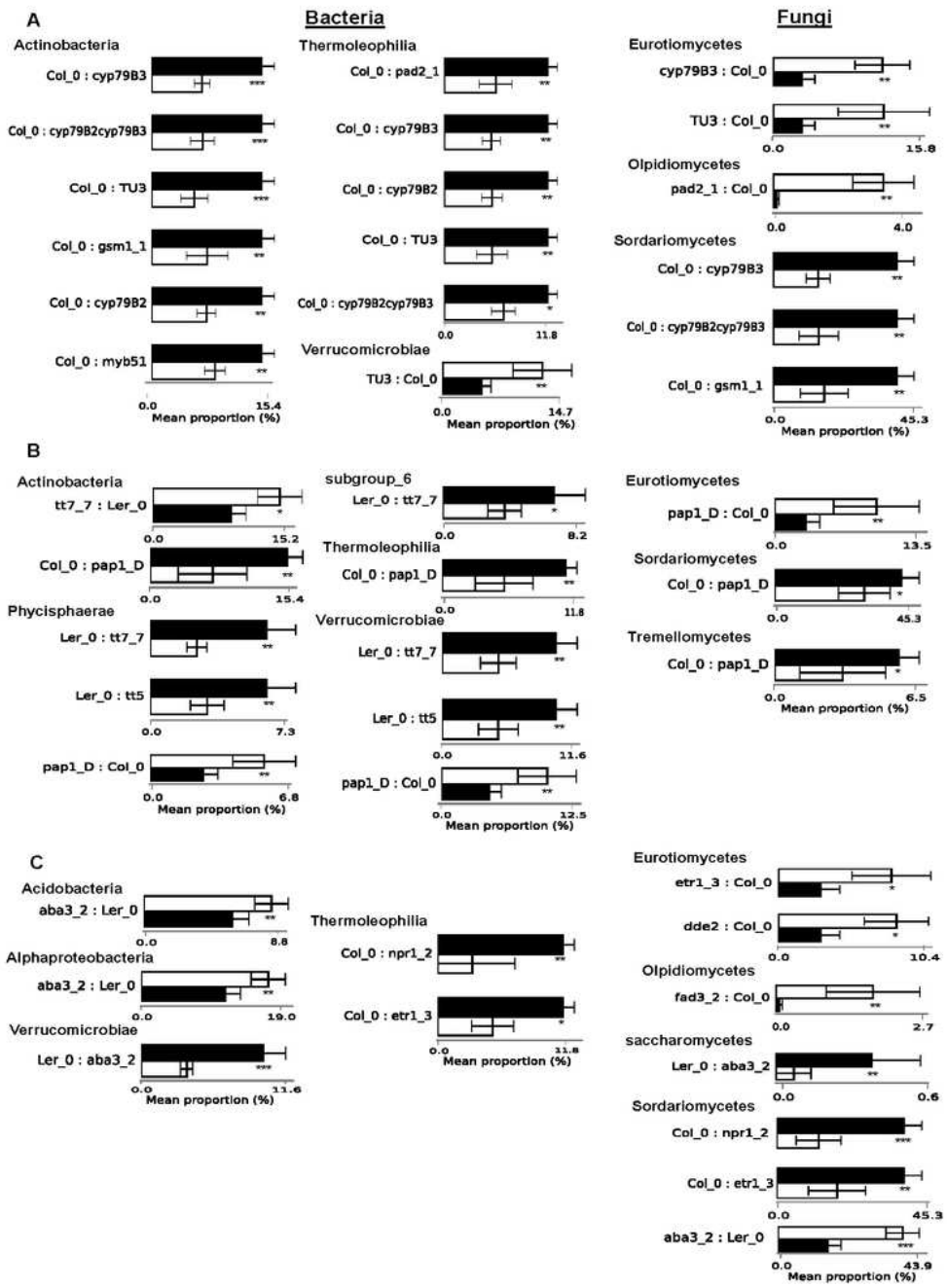

Figure 1

Bar plots showing mean distribution of reads assigned at class level in A) GLS mutants and their controls, B) FLV mutants and their controls and C) defense signaling mutants and their controls. Mutants were compared to their background controls by ANOVA, followed by the Tukey–Kramer post hoc test (p

<0.05) using the Benjamini and Hochberg (BH) FDR for multiple comparisons. Only top 10 taxa were used and taxa with small effect sizes were removed by filtering (effect size = 0.8). The black and white bar plots represent controls and mutants respectively. Error bars represent standard deviations. The analysis was performed using the STAMP software (v2.1.3)

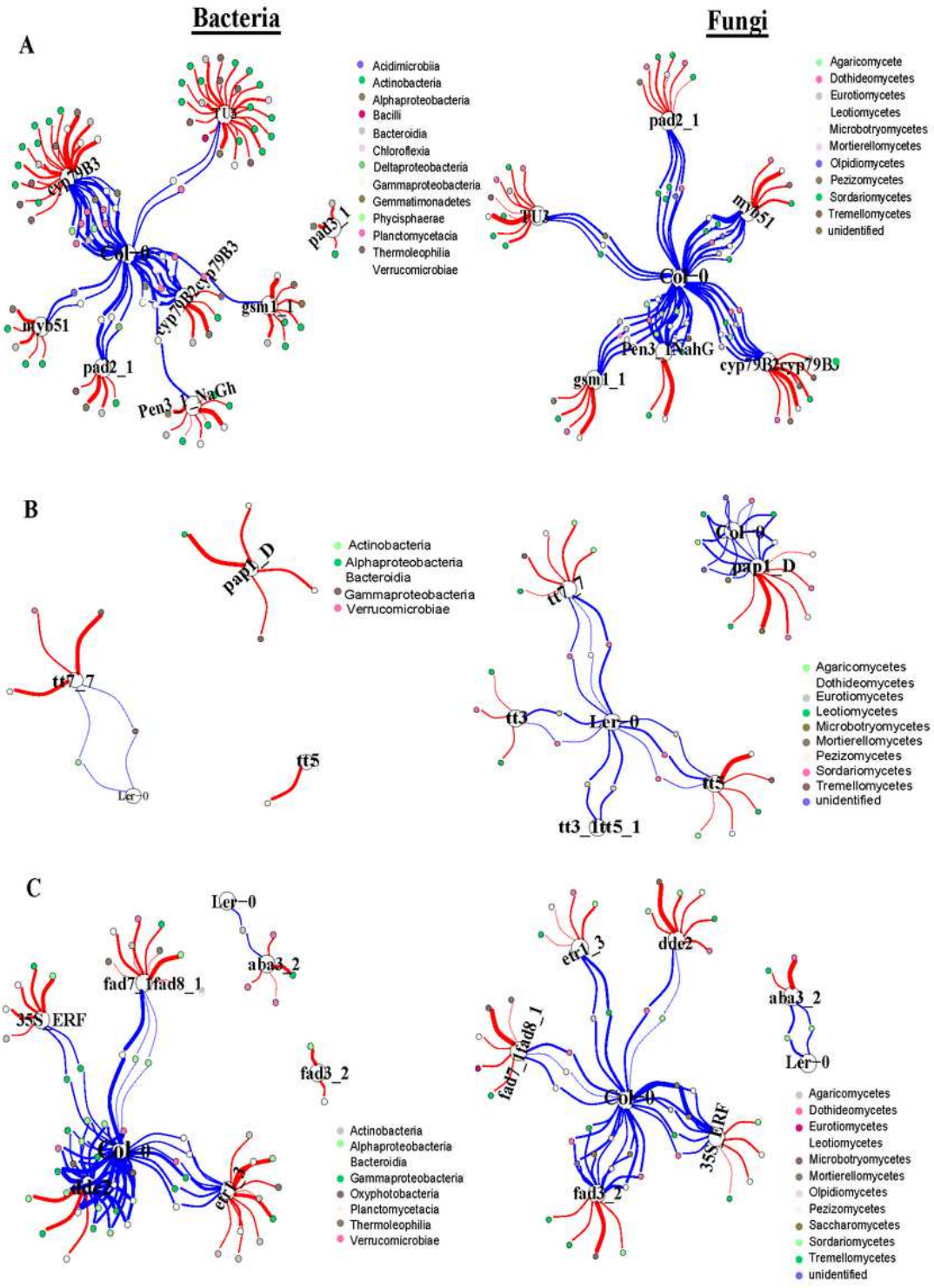

Figure 2

Network showing microbial differential analysis between mutants and controls. Bacterial and fungal genera that were significantly affected are shown for A) GLS mutants and control. B) FLV mutants and control C) defense signaling mutants and control. Analysis performed using DESeq2. Enrichment in mutants are shown in red and in blue for controls. Line width indicates the significant level of effect.

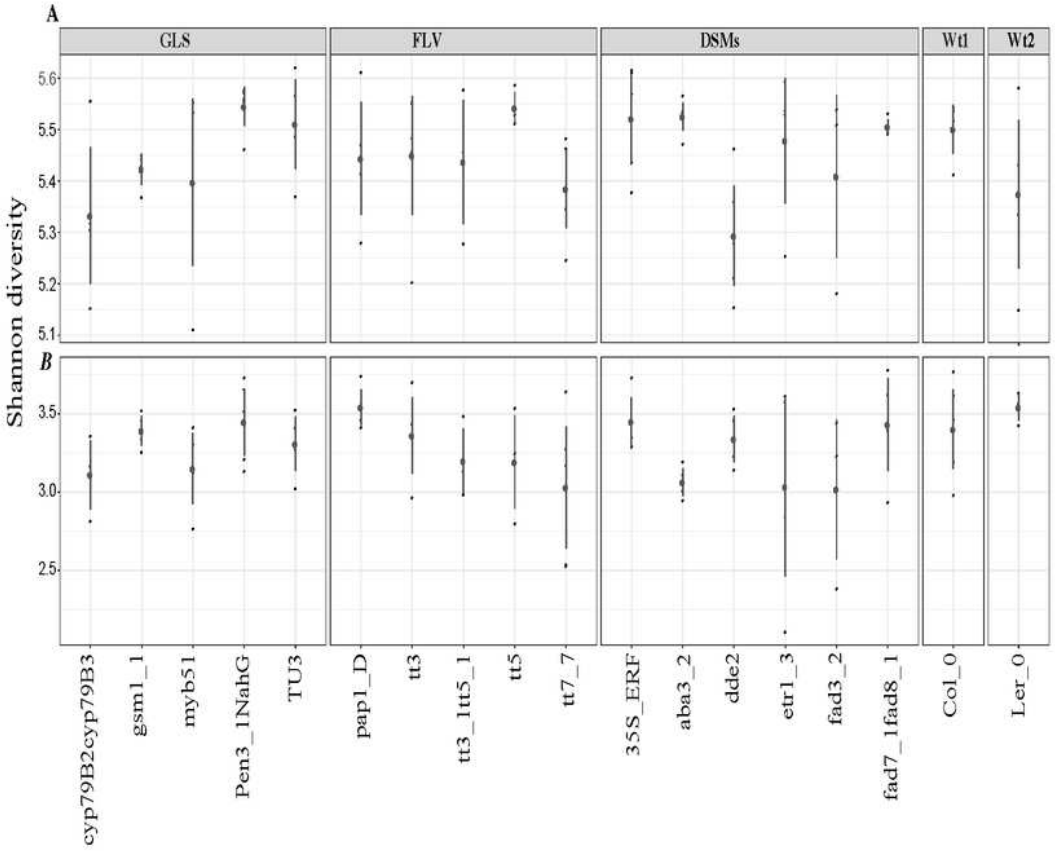

Figure 3

Alpha diversity estimated using Shannon diversity for the respective genotypes. A) Bacterial and (B) fungal Shannon diversity in different genotypes. Samples with at least 3 replicates for both bacteria and fungi (with bacterial and fungal reads >800 and >500 respectively) are shown.

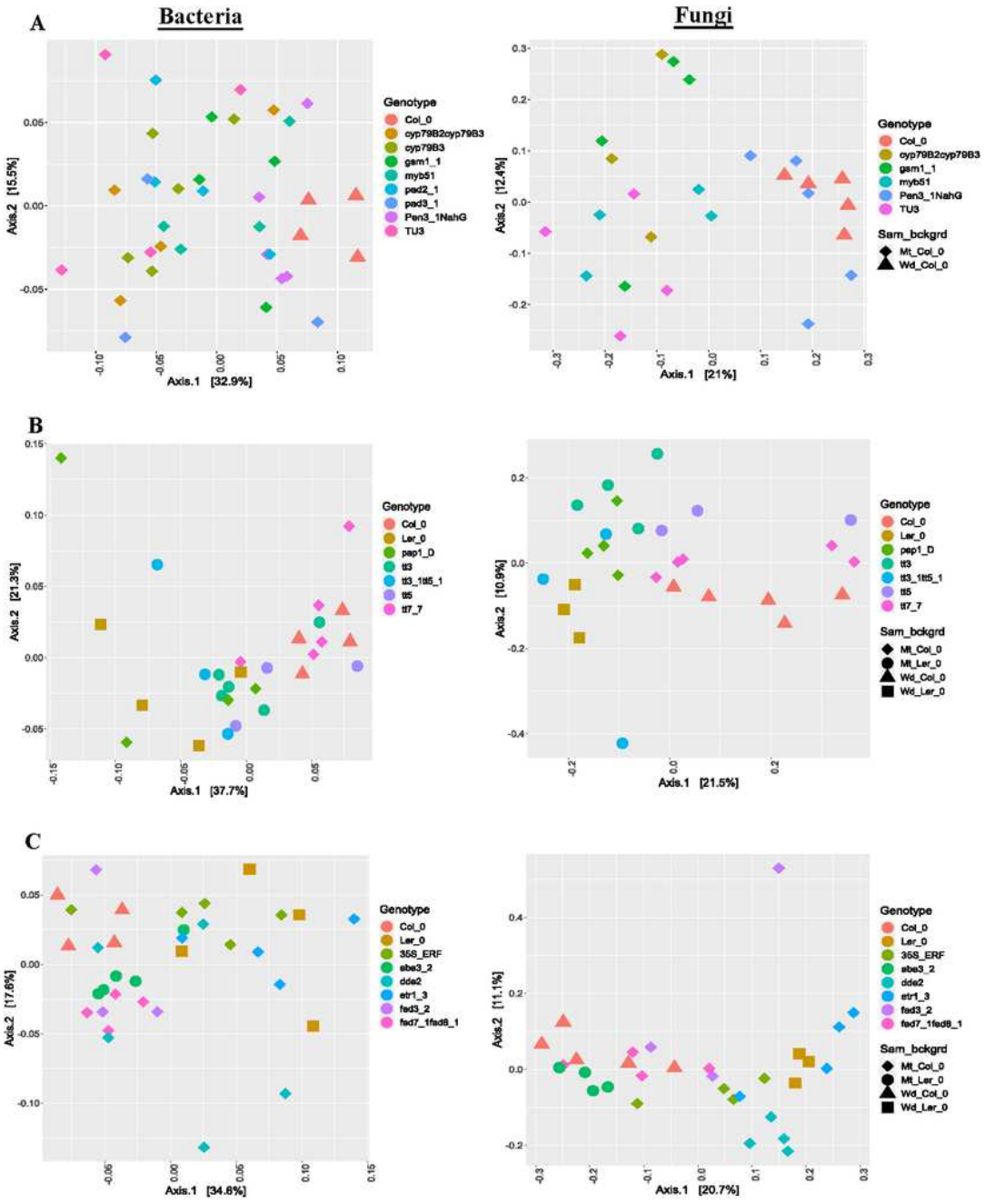

Figure 4

Principal coordinate analysis (PCoA) of weighted UniFrac distances (bacterial) and Bray- Curtis (fungal) between GLS (A), FLV (B) and DSM (C) genotypes. Individual genotypes and sample groups are shown in

different colours and shapes.

Supplementary Files

This is a list of supplementary files associated with this preprint. Click to download.

- Additionalfile1.pdf
- ST1ListofArabidopsis.docx
- ST26BacFunDESeqoutput.xlsx